Double Kill: Compressive-Sensing-Based Narrow-Band Interference and Impulsive Noise Mitigation for Vehicular Communications

Sicong Liu, *Student Member, IEEE*, Fang Yang, *Senior Member, IEEE*,
Wenbo Ding, *Student Member, IEEE*, and Jian Song, *Senior Member, IEEE*

***Abstract*—Narrow-band interference (NBI) and impulsive noise (IN) are two kinds of non-Gaussian noise that have a severe impact on vehicular communications. In this paper, a novel compressive sensing (CS)-based method of simultaneous NBI and IN mitigation is proposed, which is a *double kill* of the two kinds of unfavorable disturbances. A CS-based time–frequency-measuring orthogonal frequency-division multiplexing (CS-TFM-OFDM) frame structure is introduced, in which the temporal repeated training sequences (TSs) are exploited by the proposed CS-based differential measuring (CS-DM) method to acquire the CS measurement vector of the NBI. With the aid of the *a priori* partial support, we further proposed the *a priori*-aided sparsity adaptive matching pursuit (PA-SAMP) to improve the accuracy and stability of NBI recovery. Meanwhile, the measurement vector of the IN is acquired from the null subcarriers in the CS-TFM-OFDM frame. After partial support of the IN is obtained, the IN is reconstructed using the proposed PA-SAMP algorithm. Hence, the two categories of non-Gaussian noise are both thoroughly eliminated, leading to the stability and robustness of vehicular communications. The proposed CS-based approach outperforms the conventional noise suppression methods in vehicular communications environments, which is validated by theoretical analysis and computer simulations.**

***Index Terms*—*A priori*-aided sparsity adaptive matching pursuit (PA-SAMP), compressive sensing (CS), CS-based differential measuring (CS-DM), impulsive noise, narrow-band interference (NBI), vehicular communications.**

I. Introduction

VEHICULAR communications require a high-speed data transmission network to support the increasing demand for modern vehicular control, intelligent driving, entertainment, and other in-vehicle, vehicle-to-vehicle (V2V), or vehicle-to-grid (V2G) communication applications [1]. To avoid the extra weight, complexity, and cost of the dedicated wires for data transmission, wireless techniques [2] and power-line communications (PLC) that reuse in-vehicle power lines for data communications [1] are recently becoming popular as the technologies for vehicular communications. Orthogonal frequency-division multiplexing (OFDM) has drawn plenty of research attention [3], [4] and is widely adopted in vehicular communications for its high spectral efficiency, such as in the OFDM-based wireless systems specified by the 802.11p Wireless Access in Vehicular Environments (WAVE) standard [5] or PLC systems specified by the HomePlug Green PHY standard for V2G communications [6], etc. One important detrimental character of OFDM-based vehicular communication systems is its vulnerability to the non-Gaussian impulsive noise (IN) and narrow-band interference (NBI) [7], [8]. These two kinds of non-Gaussian noise stochastically occur in wired or wireless vehicular channels, causing severe degradation on the transmission performance, such as the performance of synchronization, demodulation, and decoding [9]–[11]. Essentially, the NBI generated by intended or unintended narrow-band signals has severe impacts on the transmitted broadband OFDM signal of interest. The IN is commonly generated by ignition noise in vehicles and the switches of electric devices which might cause transmission errors to the data frames of interest. The influences of both NBI and IN are the bottlenecks of implementing a high-speed stable vehicular communication system.

Some conventional schemes have been proposed to mitigate the NBI or IN. A frequency-domain threshold excluding (FTE) method excludes NBI contaminated subcarriers by detecting the power that exceeds the threshold [12]. A notch filter is designed at the subcarriers where NBI is located through the time-domain linear prediction approach [13]. The time-domain methods can relieve the impacts of spectral leakage with the cost of complicated design and implementation. The impacts of NBI on data subcarriers are sequentially detected and subtracted through hard decisions of OFDM data blocks in [14], although an estimation error might propagate to the subsequent detections. In terms of conventional schemes of IN mitigation, some research has focussed on the clipping and/or blanking method against the IN [15]. A multiple channel selection combining scheme to suppress the IN modeled by

Manuscript received January 31, 2015; revised May 12, 2015 and July 13, 2015; accepted July 18, 2015. Date of publication July 21, 2015; date of current version July 14, 2016. This work was supported in part by the National Natural Science Foundation of China (NSFC) under Grant 61401248 and Grant 61471219; by the Science Fund for Creative Research Groups of NSFC under Grant 61321061; the R&D Project of Science and Technology Innovation Commission of Shenzhen, China, under Grant GJHZ20130417162825486; by the New Generation Broadband Wireless Mobile Communication Network of the National Science and Technology Major Projects under Grant 2015ZX03002008; by the Tsinghua University Initiative Scientific Research Program under Grant 2014Z06098; and by the Science and Technology Project of the State Grid Corporation of China under Grant SGHAZZ00FCJS1500238. The review of this paper was coordinated by Dr. C. Xing.

The authors are with the DTV Technology R&D Center, Research Institute of Information Technology, Tsinghua National Laboratory for Information Science and Technology, Tsinghua University, Beijing 100084, China (e-mail: liu-sc12@mails.tsinghua.edu.cn; fangyang@tsinghua.edu.cn; dwb11@mails.tsinghua.edu.cn; jsong@tsinghua.edu.cn).

Color versions of one or more of the figures in this paper are available online at http://ieeexplore.ieee.org.

Digital Object Identifier 10.1109/TVT.2015.2459060

Gaussian mixture is proposed in [16]. Precoding and frequency algebraic interpolation techniques with Reed–Solomon coding and decoding are implemented to detect the positions of IN [17]. However, these conventional noise mitigation methods only combat against NBI or IN passively, which means that they are trying to suppress the noise power, nonlinearly exclude, or clip the noise contaminated data instead of reconstructing the noise and canceling them out. Hence, traditional methods result in essential performance limitation. Contrarily, this paper is pursuing the method that is able to accurately recover the noise and *double kill* them both out of the information data.

To overcome the drawbacks of the conventional schemes, a recent breakthrough in signal processing, i.e., compressive sensing (CS), can be introduced to recover the NBI and IN that are naturally sparse in the frequency and time domains, respectively. According to the CS theory, a sparse signal can be accurately recovered from the measurement vector with much smaller size than the signal dimension in the presence of background noise [18]. CS methods have been applied in many areas, such as channel estimation [19]. Nevertheless, the research on CS-based NBI or IN estimation is inadequate yet. A null space (NS) approach first introduced CS theory to NBI mitigation, in which the NS of the channel transfer matrix is calculated to obtain the measurement vector for NBI estimation [20]. The unused subcarriers are utilized as measurement vector to estimate the IN signal using the sparse convex optimization (SCO) method in [21]. To improve this method, the semi-orthogonal structure of the observation matrix is exploited to estimate the IN clusters, and the IN is estimated by computing the conditional expectation of the Gaussian mixture distribution [22]. Furthermore, to the best of the authors' knowledge, there is no related research on simultaneously recovering both the NBI and IN to ensure the stability and reliability of high-rate vehicular communications.

To solve the aforementioned problems, this paper proposes a novel simultaneous NBI and IN cancelation scheme based on CS for dependable vehicular communication systems. The CS-based time–frequency-measuring OFDM (CS-TFM-OFDM) frame structure is proposed to obtain the CS measurement vectors for NBI and IN. Under this framework, the spectral efficiency is not degraded compared with the cyclic-prefix OFDM (CP-OFDM) [23], [24] since the only difference between them is replacing the guard interval with repeated training sequences (TSs). Due to the introduction of the CS-TFM-OFDM frame structure, the difficulty in NBI measurement vector acquisition can be smoothly conquered by the proposed CS-based differential measuring (CS-DM) method that exploits the temporal repeated TSs with low complexity. The IN measurement vector is obtained from the null subcarriers in the frequency domain. Sparsity adaptive matching pursuit (SAMP) [25], which is one of the classical CS greedy algorithms, is improved and the *a priori*-aided SAMP (PA-SAMP) is then proposed with the aid of the *a priori* partial support to further improve the recovery accuracy. Hence, the NBI and IN are simultaneously and separately recovered, i.e., *double killed*. Thus, reliable vehicular data transmission is guaranteed under the proposed framework.

The remainder of this paper is organized as follows. The NBI and IN models in vehicular communication channels and the proposed CS-TFM-OFDM frame structure for NBI and IN recovery are described in Section II. Section III presents the proposed simultaneous NBI and IN recovery approach based on PA-SAMP, which is the main contribution of this paper. The performance evaluation and computational complexity analysis of the proposed approach are given in Section IV. Simulation results are demonstrated in Section V to validate the proposed approach, followed by the conclusions.

Notation: Matrices and column vectors are denoted by boldface letters. $(\cdot)^{\dagger}$ and $(\cdot)^{H}$ denote the pseudoinversion operation and conjugate transpose. $\|\cdot\|_r$ represents the ℓ_r-norm operation. $|\Gamma|$ denotes the cardinality of the set Γ. $\mathbf{v}|_{\Gamma}$ denotes the entries of vector $\mathbf{v}$ in the set of Γ. $\mathbf{A}_{\Gamma}$ represents the submatrix comprised of the Γ columns of the matrix $\mathbf{A}$. Γ^c denotes the complementary set of Γ. $\max(\mathbf{v}, T)$ denotes the indexes of the T largest entries of the vector $\mathbf{v}$. $\mathbb{E}_X\{\cdot\}$ denotes the mathematical expectation on a random variable X.

II. System Model

A. Statistical NBI Model

The frequency-domain NBI signal associated with the ith transmitted TS, which is a sparse vector $\tilde{\mathbf{e}}_i = [\tilde{e}_{i,0}, \tilde{e}_{i,1}, \ldots, \tilde{e}_{i,N-1}]^T$ in the OFDM system with N subcarriers, can be modeled by a superposition of tone interferers. Each tone interferer can be modeled by bandlimited Gaussian noise (BLGN) as described in state-of-art literature [26], [27] with its central frequency randomly distributed at all the N subcarriers (without loss of generality, other *arbitrary* random amplitude distributions are also applicable for each tone interferer), and the power spectral density (PSD) is $N_{0,\mathrm{NBI}} = \sigma_e^2$. The frequency-domain NBI is a naturally sparse vector that has only a few nonzero entries since each tone interferer is bandlimited, and the sparsity level of the NBI K_N defined by the number of nonzero entries is much smaller than the signal dimension, i.e., $K_N = |\Gamma_i| \ll N$, where $\Gamma_i = \{k | \tilde{e}_{i,k} \neq 0, k = 0, 1, \ldots, N-1\}$ is the support defined by the set of the nonzero-entry locations of the NBI signal. Accordingly, the time-domain NBI signal $\mathbf{e}_i = [e_{i,0}, e_{i,1}, \ldots, e_{i,M-1}]^T$ associated with the ith TS of length M is modeled by a superposition of independent tone interferers given by

$$e_{i,n} = \sum_{k \in \Gamma_i} \tilde{e}_{i,k} \cdot \exp\left(\frac{j2\pi kn}{N}\right), \quad n = 0, 1, \ldots, M-1. \quad (1)$$

The time-domain and frequency-domain NBI vectors are related by inverse discrete Fourier transform (IDFT) operation as $\mathbf{e}_i = \mathbf{F}_M \tilde{\mathbf{e}}_i$, and the partial IDFT matrix $\mathbf{F}_M \in \mathbb{C}^{M \times N}$ is given by

$$\mathbf{F}_M = \frac{1}{\sqrt{N}} [\boldsymbol{\gamma}_0 \quad \boldsymbol{\gamma}_1 \quad \cdots \quad \boldsymbol{\gamma}_{N-1}] \quad (2)$$

where $\boldsymbol{\gamma}_k$ is a vector with the nth element being $\exp(j2\pi kn/N), n = 0, 1, \ldots, M-1$. Usually, the interference-to-noise ratio (INR) defined as $\mathbb{E}_{\tilde{\mathbf{e}}_i}\{\mathscr{P}_N\}/\sigma_w^2$ is used as an indicator of the NBI intensity compared with the background

noise, with the average power $\mathscr{P}_N = \sum_{k\in\Gamma_i} |\tilde{e}_{i,k}|^2/K_N$ and the variance of the background additive white Gaussian noise (AWGN) σ_w^2. Since each tone interferer is a BLGN, the spectral amplitude of each tone interferer is a random Gaussian variable with the variance σ_e^2, which is equal to the value of the PSD of the BLGN. Therefore, it can be derived that $\mathbb{E}_{\tilde{\mathbf{e}}_i}\{\mathscr{P}_N\} = \sigma_e^2$, and the INR equals σ_e^2/σ_w^2. Without loss of generality, the NBI support can be randomly distributed and the sparsity level is different correspondingly [28], [29], which is applied to the practical vehicular communication channels.

The NBI signal in vehicular communications generally comes from the licensed services (e.g., Bluetooth) to IEEE 802.11a/g/n systems sharing the same band [10] and inappropriate spectrum allocation plans of amateur radio ingress [5], electrical onboard devices, or broadcasting interferers [30] that are working at relatively fixed frequencies during the period that is longer than the duration of adjacent consecutive frames. Hence, there exist temporal correlation of the NBI, i.e., the support and amplitudes of the NBI signal can be treated as quasi-static within the duration of two adjacent OFDM data blocks [31], [32]. As will be explained in detail in Section III, the temporal correlation will facilitate the proposed CS-DM method since the repeated TSs at adjacent received frames could be used to cancel out the TS component and obtain the CS measurement vector. In addition, the estimated NBI at the TS can be exploited to recover the NBI at the corresponding OFDM data block.

B. Statistical IN Model

The IN vector associated with the ith OFDM data block is denoted by $\boldsymbol{\xi}_i = [\xi_{i,0}, \xi_{i,1}, \ldots, \xi_{i,N-1}]^T$ of length N. One of its fundamental features is that the IN vector is sparse, with the support $\Pi_i = \{j|\xi_{i,j} \neq 0,\ j = 0, 1, \ldots, N-1\}$ and sparsity level $K_I = |\Pi_i|$. The INR is represented by $\mathscr{P}_I/\sigma_w^2$, where $\mathscr{P}_I = \sum_{j\in\Pi_i} |\xi_{i,j}|^2/K_I$ is the average power of IN. The statistical properties of the instantaneous amplitude and the random occurrence of IN have been empirically modeled in literature, mainly including the Gaussian mixture [33] and the Middleton's Class A models [34].

The instantaneous amplitude of the time-domain asynchronous IN that is commonly encountered in vehicular communications can be modeled by the Gaussian mixture distribution [33], with the probability density function (pdf) given by

$$p_Z(z) = \sum_{j=0}^{J_m} \beta_j \cdot g_j(z) \tag{3}$$

where $g_j(z)$ is the pdf of Gaussian distribution with zero mean and variance σ_j^2, β_j is the mixture coefficient of the corresponding Gaussian pdf, and J_m is the number of Gaussian components.

The Middleton's Class A model is a common statistical model of IN with the parameters of the overlapping factor A and the background-to-impulsive-noise power ratio ω [34]. Gaussian mixture distribution can generate its special-case Middleton's Class A distribution when the parameters $\beta_j = e^{-A}A^j/j!$ and $\sigma_j^2 = (j/A + \omega)/(1+\omega)$ as $J_m \to \infty$.

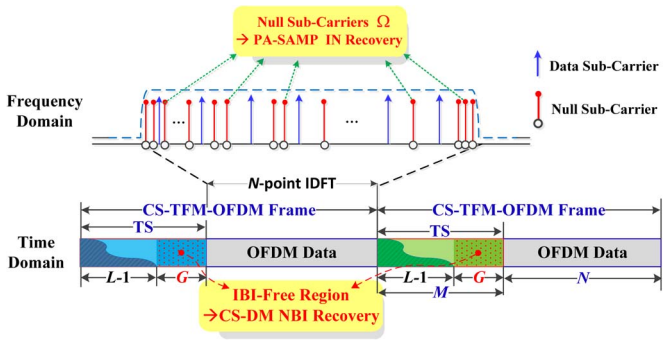

Fig. 1. Time–frequency frame structure of CS-TFM-OFDM exploited for CS-based NBI and IN cancelation for vehicular communications.

The arrival rate of the IN bursts, i.e., the number of the IN bursts per second, follows the Poisson process given by

$$P(\Lambda) = \frac{\lambda^\Lambda e^{-\lambda}}{\Lambda!} \tag{4}$$

where λ denotes the rate of IN arrivals [35]. The Middleton's Class A model and the Poisson process arrival model are adopted in this paper.

C. System Model of CS-TFM-OFDM

In conventional wireless or wired vehicular communication systems, each frame in the payload is usually prefixed by its CP, such as in the IEEE 802.11p WAVE and the HomePlug Green PHY standards [5], [6]. In this paper, we introduce the CS-TFM-OFDM frame structure to provide the temporal repeated TSs that are taken full advantage of by the proposed CS-DM method. The repeated TSs have already been adopted as guard intervals in digital terrestrial television broadcasting (DTTB) specified in [36] for channel estimation, synchronization, etc. Meanwhile, the null subcarriers, including the reserved tones and the virtual mask subcarriers specified in the state-of-the-art standards such as IEEE 802.11p and HomePlug Green PHY [5], [6], are utilized to acquire the measurement vector of IN under the proposed CS-TFM-OFDM framework.

The proposed CS-TFM-OFDM frame structure applied in typical vehicular communication systems is shown in Fig. 1. In the time domain, the ith frame $\mathbf{s}_i = [\mathbf{c}^T \quad \mathbf{x}_i^T]^T$ consists of the constant TS $\mathbf{c} = [c_0, c_1, \ldots, c_{M-1}]^T$ of length M and the following OFDM data block $\mathbf{x}_i = [x_{i,0}, x_{i,1}, \ldots, x_{i,N-1}]^T$ of length N, where the TSs for different frames are identical. The ith time-domain OFDM data block is the IDFT of the related frequency-domain data in the N subcarriers, which contains a set of reserved null subcarriers denoted by the set Ω. Then, the transmitted signal passes through the multipath vehicular channel with the channel impulse response (CIR) of $\mathbf{h}_i = [h_{i,0}, h_{i,1}, \ldots, h_{i,L-1}]^T$ with length L in the presence of the NBI $\tilde{\mathbf{e}}_i$, the IN $\boldsymbol{\xi}_i$, and AWGN $\mathbf{z}_i$.

At the receiver, the time-domain received TS $\mathbf{y}_i = [y_{i,0}, y_{i,1}, \ldots, y_{i,M-1}]^T$ can be presented as

$$\mathbf{y}_i = \boldsymbol{\Phi}_M \mathbf{h}_i + \mathbf{F}_M \tilde{\mathbf{e}}_i + \mathbf{z}_i \tag{5}$$

where the TS component at the receiver is denoted by $\mathbf{\Phi}_M \mathbf{h}_i$, with the matrix $\mathbf{\Phi}_M \in \mathbb{C}^{M\times L}$ represented by

$$\mathbf{\Phi}_M = \begin{bmatrix} c_0 & x_{i-1,N-1} & x_{i-1,N-2} & \cdots & x_{i-1,N-L+1} \\ c_1 & c_0 & x_{i-1,N-1} & \cdots & x_{i-1,N-L+2} \\ c_2 & c_1 & c_0 & \cdots & x_{i-1,N-L+3} \\ \vdots & \vdots & \vdots & \ddots & \vdots \\ c_{L-2} & c_{L-3} & c_{L-4} & \cdots & x_{i-1,N-1} \\ c_{L-1} & c_{L-2} & c_{L-3} & \cdots & c_0 \\ c_L & c_{L-1} & c_{L-2} & \cdots & c_1 \\ \vdots & \vdots & \vdots & \ddots & \vdots \\ c_{M-1} & c_{M-2} & c_{M-3} & \cdots & c_{M-L} \end{bmatrix}$$

whose entries $\{x_{i-1,n}\}_{n=N-L+1}^{N-1}$ represent the last $L-1$ samples of the $(i-1)$th OFDM data block $\mathbf{x}_{i-1}$, which causes interblock interference (IBI) on the ith TS. Since the $(i-1)$th OFDM data block $\mathbf{x}_{i-1}$ only causes IBI on the first $L-1$ samples of the ith received TS $\mathbf{y}_i$, the last $G = M-L+1$ samples of $\mathbf{y}_i$ will form the *IBI-free* region $\mathbf{q}_i = [y_{i,L-1}, y_{i,L}, \ldots, y_{i,M-1}]^T$ denoted by

$$\mathbf{q}_i = \mathbf{\Phi}_G \mathbf{h}_i + \mathbf{F}_G \tilde{\mathbf{e}}_i + \mathbf{w}_i \tag{6}$$

where $\mathbf{q}_i$ consists of the last G elements of $\mathbf{y}_i$, whereas $\mathbf{F}_G$ and $\mathbf{\Phi}_G$ are the $G \times N$ observation matrix composed of the last G rows of $\mathbf{F}_M$, and the $G \times L$ Toeplitz matrix composed of the last G rows of $\mathbf{\Phi}_M$, respectively. $\mathbf{w}_i$ denotes the AWGN vector related to the IBI-free region with zero mean and the variance of σ_w^2. The IBI-free region exists in practical vehicular communication systems because a common rule for the system design is to configure the guard interval length M to be larger than the maximum channel length L in the worst case to avoid IBI between OFDM data blocks [36], [37]; therefore, L is usually smaller than M, i.e., $L < M$.

In the frequency domain at the receiver, as shown in Fig. 1, the received data in the reserved null-subcarrier set Ω are denoted by

$$\tilde{\mathbf{p}}_i = \mathbf{F}_R \boldsymbol{\xi}_i + \tilde{\mathbf{w}}_i \tag{7}$$

where the vector $\tilde{\mathbf{p}}_i = [\tilde{p}_{i,0}, \tilde{p}_{i,1}, \ldots, \tilde{p}_{i,R-1}]^T$ of length $R = |\Omega|$ is the measurement vector of the IN at the null subcarriers, and $\tilde{\mathbf{w}}_i$ denotes the corresponding frequency-domain AWGN vector, whereas the observation matrix to be used for the CS-based IN recovery is the partial discrete Fourier transform (DFT) matrix $\mathbf{F}_R$ given by

$$\mathbf{F}_R = \frac{1}{\sqrt{N}} [\boldsymbol{\chi}_0 \quad \boldsymbol{\chi}_1 \quad \cdots \quad \boldsymbol{\chi}_{N-1}] \tag{8}$$

where the kth entry of $\boldsymbol{\chi}_m$ is $\exp(-j2\pi mk/N), k \in \Omega, m = 0, \ldots, N-1$. The measurement vector $\tilde{\mathbf{p}}_i$ at the set Ω contains the IN component and the background AWGN, whereas the OFDM data component is not included since the null subcarriers are set to zeros at the transmitter.

III. Simultaneous Narrow-Band Interference and Impulsive Noise Reconstruction Based on *A Priori*-Aided Compressive Sensing

A. NBI Reconstruction Using CS-DM

1) CS-DM Approach for NBI Recovery: Under the CS framework, it is important to acquire the measurement vector for CS-based recovery of the sparse NBI signal [18]. The measurement vector is supposed to contain the NBI component. However, the data or TS components are mixed up with the NBI in the measurement vector and should be nulled out to improve the performance of CS-based recovery. After their removal, the remaining background AWGN will have an influence on the CS recovery performance. Nevertheless, it is proved in [38] that it is highly probable to recover the sparse signal accurately in the presence of the power-constrained background AWGN noise. The effect of the AWGN power (indicated by INR) is analyzed in the following proposed method and shown in simulations in Section V.

It is noted from (6) that the TS component $\mathbf{\Phi}_G \mathbf{h}_i$ is supposed to be nulled out to acquire the measurement vector, which contains the NBI component with only AWGN. Unlike the conventional method that utilizes the NS to acquire the measurement vector, a novel CS-DM method is proposed to obtain the measurement vector of the NBI. Usually, when the channel is not varying so fast, the CIRs for adjacent frames keep approximately invariant [39], i.e., $\mathbf{h}_i \approx \mathbf{h}_{i+1} = \mathbf{h}$, since the distance between the two frames is sufficiently small so that the duration is within the channel coherence time. Hence, the TS component $\mathbf{\Phi}_G \mathbf{h}_i$ can be simply eliminated by subtracting $\mathbf{q}_{i+1}$ from $\mathbf{q}_i$ given in (6), i.e., through the differential operation between the IBI-free regions of the adjacent received TSs, which yields the measurement vector $\Delta\mathbf{q}_i$ or the CS measurement, i.e.,

$$\Delta\mathbf{q}_i = \mathbf{F}_G \Delta\tilde{\mathbf{e}}_i + \Delta\mathbf{w}_i \tag{9}$$

where $\Delta\mathbf{q}_i = \mathbf{q}_i - \mathbf{q}_{i+1}, \Delta\mathbf{w}_i = \mathbf{w}_i - \mathbf{w}_{i+1}$, and the NBI differential vector $\Delta\tilde{\mathbf{e}}_i \in \mathbb{C}^N$ is denoted as follows:

$$\Delta\tilde{\mathbf{e}}_i = \tilde{\mathbf{e}}_i - \tilde{\mathbf{e}}_{i+1} = [\Delta\tilde{e}_{i,0}, \Delta\tilde{e}_{i,1}, \ldots, \Delta\tilde{e}_{i,N-1}]^T. \tag{10}$$

Due to the temporal correlation of the NBI, it can be noted that the time-domain NBI vector at the $(i+1)$th TS $\mathbf{e}_{i+1}$ equals that of the ith TS $\mathbf{e}_i$ delayed by Δl samples, where $\Delta l = M + N$ is the distance between the two TSs. Hence, there is a relation that the frequency-domain NBI vector at the $(i+1)$th TS $\tilde{\mathbf{e}}_{i+1}$ equals $\tilde{\mathbf{e}}_i$ with a phase shift, i.e., $\tilde{e}_{i+1,k} = \tilde{e}_{i,k} \exp(j2\pi k\Delta l/N), k = 0, 1, \ldots N-1$, which facilitates the CS-DM of the NBI. Therefore, the entries of the NBI differential vector in (10) are given by

$$\Delta\tilde{e}_{i,k} = \tilde{e}_{i,k} \left(1 - \exp\left(\frac{j2\pi k\Delta l}{N}\right)\right), \; k = 0, 1, \ldots, N-1. \tag{11}$$

To completely avoid any possible influence of IN on the CS-DM approach for NBI recovery, the measurement vector of the NBI $\Delta\mathbf{q}_i$ can be refined by excluding the measurement samples that are possible to be affected by IN, i.e., excluding

the samples with the power exceeding the power threshold as follows:

$$\eta_t = \alpha \cdot \frac{1}{G} \sum_{m=1}^{G} |\Delta q_{i,m}|^2 \tag{12}$$

where α is a scaling coefficient given by $\alpha = \sqrt{\sum_{j\in\Pi_i} |\xi_{i,j}|^2/(2\sigma_w^2 K_I)}$ to ensure the accuracy of excluding IN contaminated samples and to avoid mislabeled samples affected by IN. With the refined measurement vector $\Delta\mathbf{q}_i$, the unknown sparse NBI differential vector $\Delta\tilde{\mathbf{e}}_i$ will be reconstructed after solving (9) using the CS algorithms [18], [38]. Due to its temporal correlation, the NBI estimation associated with the TS can be used to obtain the NBI of the subsequent OFDM data block in the same frame without loss of accuracy.

Solving the underdetermined CS measurement (9) is equivalent to solving the convex optimization problem given by

$$\min_{\Delta\tilde{\mathbf{e}}_i\in\mathbb{C}^N} \|\Delta\tilde{\mathbf{e}}_i\|_1, \quad \text{s.t. } \|\Delta\mathbf{q}_i - \mathbf{F}_G\Delta\tilde{\mathbf{e}}_i\|_2 \le \varepsilon_N \tag{13}$$

where ε_N is the bound of the ℓ_2 constraint due to the AWGN $\Delta\mathbf{w}_i$ in (9) and is set according to the AWGN distribution [38]. The problem in (13) can be solved by convex programming methods such as basis pursuit (BP) in the literature [40], but in some parameter regimes, BP is inefficient, and its implementation cost is high. Furthermore, (13) can be more efficiently solved using classical CS greedy algorithms, such as the orthogonal matching pursuit (OMP) [41], subspace pursuit (SP) [42], and SAMP [25]. However, some famous greedy algorithms, such as OMP and SP, require the sparsity level to be known, which is not realistic since the NBI model is variable and unknown at the receiver. Hence, the SAMP algorithm that is adaptive to unknown and variable sparsity levels is applied in this paper. However, the performance of SAMP might degrade in severe conditions. To deal with this, the performance of SAMP is further improved by the proposed PA-SAMP algorithm with the aid of the partial support, as described in detail in the following.

2) NBI Partial Support A Priori Acquisition: It is necessary for the NBI partial support, i.e., the *a priori* information, to be first acquired and utilized to facilitate the NBI recovery process and improve the accuracy of the CS algorithm.

From (9), it is observed that the measurement vector only contains the NBI component and background AWGN, without the disturbance of TS or data components. The N-point DFT of the measurement vector $\Delta\tilde{\mathbf{q}}_i = [\Delta\tilde{q}_{i,0}, \Delta\tilde{q}_{i,1}, \ldots, \Delta\tilde{q}_{i,N-1}]$ contains some partial information of the NBI support, with some spectral leakage because the measurement vector length G is smaller than N. However, the intensity of the NBI is commonly much higher than that of AWGN, which improves the resolution of the NBI locations in the spectrum of $\Delta\tilde{\mathbf{q}}_i$. Hence, it is feasible to obtain the estimation of the NBI partial support $\Gamma^{(0)}$ at the ith frame through thresholding. The subcarriers with power exceeding the power threshold λ_f are included in the partial support $\Gamma^{(0)}$, which is given by

$$\Gamma_0 = \left\{k \,\middle|\, |\Delta\tilde{q}_{i,k}|^2 > \lambda_f,\ k = 0, 1, \ldots, N-1\right\} \tag{14}$$

where the power threshold λ_f is given by

$$\lambda_f = \frac{\beta}{N} \sum_{k=0}^{N-1} |\Delta\tilde{q}_{i,k}|^2 \tag{15}$$

where β is a scaling coefficient that can be configured proportional to the INR in different scenarios and is empirically given by $\beta = \sqrt{2\sigma_e^2/\sigma_w^2}$ as an appropriate choice that offers a proper tradeoff between complexity and accuracy. This is intuitively understandable because, when the INR is high, the threshold should become larger to avoid support that is too aggressive and that might include extra false entries. On the other hand, smaller INR will drive the threshold to become smaller to include more true entries in the partial support, i.e., to make the support less conservative, to avoid complexity increase. The *a priori* partial NBI support will help improve the performance of the CS algorithm for NBI recovery, particularly in bad conditions where the INR is relatively lower or the sparsity level K_N is larger.

3) A Priori-Aided SAMP Algorithm: With the aid of the *a priori* partial support, we propose the PA-SAMP algorithm whose pseudocode is summarized in **Algorithm 1**. The input contains the measurement vector $\Delta\mathbf{q}_i$, the observation matrix $\mathbf{\Psi} = \mathbf{F}_G$, the *a priori* partial support $\Gamma^{(0)}$, and the iteration step size Δs that can be a compromise between the convergence rate and the accuracy. During the iterations that consist of multiple stages, the testing sparsity level for the current stage is T, which is increased by Δs when the stage switches. The output is the final support Γ_i and the recovered differential NBI vector $\Delta\hat{\mathbf{e}}_i$ s.t. $\Delta\hat{\mathbf{e}}_i|_{\Gamma_i} = \mathbf{\Psi}^{\dagger}_{\Gamma_i}\Delta\mathbf{q}_i, \Delta\hat{\mathbf{e}}_i|_{\Gamma_i^c} = \mathbf{0}$.

Algorithm 1 PA-SAMP for NBI Recovery

Input:
1) *A priori* partial support $\Gamma^{(0)}$
2) Initial sparsity level $K_N^{(0)} = |\Gamma^{(0)}|$
3) Measurement vector $\Delta\mathbf{q}_i$
4) Observation matrix $\mathbf{\Psi} = \mathbf{F}_G$
5) Step size Δs.

Initialization:

$\Delta\hat{\mathbf{e}}_i^{(0)}|_{\Gamma^{(0)}} \leftarrow \mathbf{\Psi}^{\dagger}_{\Gamma^{(0)}}\Delta\mathbf{q}_i$
$\mathbf{r}^{(0)} \leftarrow \Delta\mathbf{q}_i - \mathbf{\Psi}\Delta\hat{\mathbf{e}}_i^{(0)}$
$T \leftarrow \Delta s + K_N^{(0)}, \ \ k \leftarrow 1, \ \ j \leftarrow 1$

Iterations:

repeat
  $S_k \leftarrow \max(\mathbf{\Psi}^H\mathbf{r}^{(k-1)}, T - K_N^{(0)})$ {Preliminary test}
  $C_k \leftarrow \Gamma^{(k-1)} \cup S_k$ {Make candidate list}
  $\Gamma_t \leftarrow \max(\mathbf{\Psi}^{\dagger}_{C_k}\Delta\mathbf{q}_i, T)$ {Temporary final list}
  $\Delta\hat{\mathbf{e}}_i^{(k)}|_{\Gamma_t} \leftarrow \mathbf{\Psi}^{\dagger}_{\Gamma_t}\Delta\mathbf{q}_i, \Delta\hat{\mathbf{e}}_i^{(k)}|_{\Gamma_t^c} \leftarrow \mathbf{0}$
  $\mathbf{r} \leftarrow \Delta\mathbf{q}_i - \mathbf{\Psi}_{\Gamma_t}\mathbf{\Psi}^{\dagger}_{\Gamma_t}\Delta\mathbf{q}_i$ {Compute residue}
  if $\|\mathbf{r}\|_2 \ge \|\mathbf{r}^{(k-1)}\|_2$ **then**
    $j \leftarrow j+1, T \leftarrow K_N^{(0)} + j \times \Delta s$ {Stage switching}
  else
    $\Gamma^{(k)} \leftarrow \Gamma_t, \Gamma_i \leftarrow \Gamma_t, \mathbf{r}^{(k)} \leftarrow \mathbf{r}$,

14: $k \leftarrow k+1$ {Same stage, next iteration}
15: **end if**
16: **until** $\|\mathbf{r}\|_2 < \varepsilon_N$
Output:
1) Final support Γ_i
2) Recovered differential NBI vector $\Delta\hat{\mathbf{e}}_i$ s.t. $\Delta\hat{\mathbf{e}}_i|_{\Gamma_i} = \mathbf{\Psi}^{\dagger}_{\Gamma_i}\Delta\mathbf{q}_i$, $\Delta\hat{\mathbf{e}}_i|_{\Gamma_i^c} = \mathbf{0}$

It is noted from **Algorithm 1** that the partial support $\Gamma^{(0)}$ in PA-SAMP is first exploited to reduce the complexity of the total iterations compared with that of SAMP. During the iterations, the accuracy of the temporary support estimation is also improved, and the complexity is reduced at each iteration. Basically, the proposed PA-SAMP is distinguished from the classical SAMP, mainly in these three aspects.

Complexity: The initial support is set as $\Gamma^{(0)}$ in PA-SAMP instead of an empty set $\emptyset$ used in SAMP, leading to the different initialization of $\Delta\hat{\mathbf{e}}_i^{(0)}|_{\Gamma^{(0)}}$ and $\mathbf{r}^{(0)}$. The testing sparsity level T is initialized as $T \leftarrow \Delta s + K_N^{(0)}$; therefore, there are only $K_N - K_N^{(0)}$ remaining nonzero entries. The average number of total iterations is reduced from K_N in SAMP to $K_N - K_N^{(0)}$ in PA-SAMP. Meanwhile, the convergence rate of the iterations is also improved since the testing sparsity level starts much closer to the actual one.

Accuracy: The *a priori*-aided initialization in PA-SAMP is more accurate than the trivial initialization in SAMP. During the stage switching, the testing sparsity level is changed to $T \leftarrow K_N^{(0)} + j \times \Delta s$ instead of $T \leftarrow j \times \Delta s$ in SAMP. Thus, it is possible to adopt smaller step size Δs in PA-SAMP, which leads to more accurate estimation of the actual sparsity level K_N.

Adaptivity: Under different channel conditions, the *a priori* input of PA-SAMP will vary accordingly because the threshold given by (15) is adjusted due to the variation of sparsity level and INR. Then, the updated partial support will facilitate the proposed PA-SAMP method to recover the latest NBI more accurately, which makes it more adaptive to the NBI variation than the conventional SAMP method. In addition, with the aid of the *a priori* information, PA-SAMP requires less measurement data to reach the accurate reconstruction criterion and thus outperforms SAMP if the length of IBI-free region is short under long channel delay; therefore, PA-SAMP is more adaptive to channel variations.

B. IN Reconstruction from Null Subcarriers

1) CS-based Measurement for IN Recovery: Recall that the measurement vector of IN $\tilde{\mathbf{p}}_i$ and the observation matrix $\mathbf{F}_R$ have been acquired from the null subcarriers in (7); it is feasible to recover the IN vector $\boldsymbol{\xi}_i$ in the presence of background AWGN $\tilde{\mathbf{w}}_i$ based on the CS theory, as described earlier from the CS equation (7).

Before solving the CS problem to recover the IN, in order to eliminate the probable influence of the NBI on the CS-based IN recovery, it is necessary to exclude the NBI contaminated subcarriers with power exceeding the given threshold η_f from the null-subcarrier set Ω, with the threshold given by

$$\eta_f = \frac{\beta^2}{R}\sum_{k=0}^{R-1}|\tilde{p}_{i,k}|^2 \tag{16}$$

where β is given in (15). At the null-subcarrier set Ω, if there happens to be an NBI contaminated subcarrier, it will be correctly detected and excluded by this thresholding procedure because the intensity of the NBI is much higher than that of the frequency-domain component of IN (due to the DFT property) and the background AWGN. Therefore, the null-subcarrier set Ω can be refined to Ω' by excluding these possibly NBI contaminated null subcarriers, and the measurement vector $\tilde{\mathbf{p}}_i$ is refined accordingly by excluding the corresponding entries.

From the refined measurement vector $\tilde{\mathbf{p}}_i$, the unknown sparse IN vector $\boldsymbol{\xi}_i$ will be reconstructed by solving the CS problem (7). Similar to the analysis of CS-based NBI recovery, solving the CS measurement equation (7) is also equivalent to solving the convex optimization problem, i.e.,

$$\min_{\boldsymbol{\xi}_i \in \mathbb{C}^N} \|\boldsymbol{\xi}_i\|_1, \quad \text{s.t. } \|\tilde{\mathbf{p}}_i - \mathbf{F}_R\boldsymbol{\xi}_i\|_2 \le \varepsilon_I \tag{17}$$

where ε_I is the bound of the ℓ_2 constraint due to the AWGN $\tilde{\mathbf{w}}_i$ in (7). Problem (17) can also be efficiently solved by classical CS algorithms, such as SP or SAMP. Since the IN in practical vehicular communication systems is variable and unknown at the receiver, SAMP is also more appropriate. Moreover, with the aid of the *a priori* partial support of the IN, the performance of SAMP can be also further improved by using the PA-SAMP algorithm described previously.

2) IN Partial Support A Priori Acquisition: The *a priori* information of the IN partial support will also improve the performance of CS-based IN recovery. Since the intensity of IN is normally much higher than that of the time-domain data component or AWGN [22], it is feasible to obtain the IN partial support Π_0 at the ith OFDM data block through the thresholding operation of the received time-domain OFDM data block $\mathbf{x}_i$. The time-domain samples with power exceeding the given threshold λ_t are included in the partial support Π_0, which is given by

$$\Pi_0 = \left\{ n \,\middle|\, |x_{i,n}|^2 > \lambda_t,\ n = 0, 1, \ldots, N-1 \right\} \tag{18}$$

where the power threshold λ_t is given by

$$\lambda_t = \alpha \cdot \frac{1}{N}\sum_{n=0}^{N-1}|x_{i,n}|^2 \tag{19}$$

where α is a given in (12). The IN partial support is able to improve the performance of the CS algorithm for IN recovery, particularly in severe conditions where the INR is relatively low or the sparsity level of IN is large.

3) IN Recovery using PA-SAMP: With the aid of the IN partial support Π_0, the original IN vector $\boldsymbol{\xi}_i$ associated with the ith OFDM data block is able to be efficiently and accurately recovered using the proposed PA-SAMP algorithm.

The detailed algorithm of PA-SAMP used for IN recovery is similar to that used for NBI recovery as explained in **Algorithm 1**. The difference is that the input, output, and the relevant parameters should be configured to those related to the IN. Specifically, the input includes the measurement vector $\tilde{\mathbf{p}}_i$, the observation matrix $\mathbf{F}_R$, and the partial support Π_0, and the iteration step size Δs. The output is the final support Π_i and the recovered IN vector $\hat{\boldsymbol{\xi}}_i$, s.t. $\hat{\boldsymbol{\xi}}_i|_{\Pi_i} = (\mathbf{F}_R)^{\dagger}_{\Pi_i}\tilde{\mathbf{p}}_i$, $\hat{\boldsymbol{\xi}}_i|_{\Pi_i^c} = \mathbf{0}$.

Afterwards, using the proposed PA-SAMP algorithm, the original IN vector $\hat{\boldsymbol{\xi}}_i$ is accurately recovered with low complexity. With the aid of the *a priori* information, this approach is also very adaptive to the variation of sparsity levels and different INRs.

C. Final Cancellation of NBI and IN

Until now, we have successfully recovered the differential NBI vector $\Delta\hat{\mathbf{e}}_i$ and the IN vector $\hat{\boldsymbol{\xi}}_i$. Afterward, the original frequency-domain NBI vector $\tilde{\mathbf{e}}_i$ at the ith TS can be reconstructed from the recovered differential NBI vector $\Delta\hat{\mathbf{e}}_i$ according to (11) by

$$\tilde{e}_{i,k} = \frac{\Delta\hat{e}_{i,k}}{\left(1 - \exp\left(\frac{j2\pi k\Delta l}{N}\right)\right)},\ k = 0, 1, \ldots, N-1. \quad (20)$$

Then, the frequency-domain NBI vector associated with the ith OFDM data block $\tilde{\mathbf{e}}_i^D = [\tilde{e}_{i,0}^D, \tilde{e}_{i,1}^D, \ldots, \tilde{e}_{i,N-1}^D]^T$ is similarly obtained by

$$\tilde{e}_{i,k}^D = \tilde{e}_{i,k} \cdot \exp\left(\frac{j2\pi k\Delta d}{N}\right),\ k = 0, 1, \ldots, N-1 \quad (21)$$

where $\Delta d = M$ is the distance between the ith TS and the ith OFDM data block. Meanwhile, the time-domain IN vector associated with the ith OFDM data block is the IN vector $\hat{\boldsymbol{\xi}}_i$ recovered by the CS-based PA-SAMP algorithm.

Finally, the frequency-domain NBI and the time-domain IN can be both eliminated separately from the received OFDM data block and be processed by the successive modules at the receiver. The *double kill* of the two noises is hereby accomplished; thus, a more reliable vehicular communication system is ensured.

IV. Performance Evaluation

A. Computational Complexity Analysis

The computational complexity of the proposed CS-based approach for NBI cancelation mainly includes the following three parts: 1) CS-DM (the complexity of the CS measurement vector acquisition is $\mathcal{O}(G)$); 2) *a priori* information acquisition (the complexity is from the fast Fourier transform process, i.e., $\mathcal{O}(N\log_2(N))$; and 3) PA-SAMP (the CS algorithm contributes the major complexity). For each iteration, the complexity consists of two parts: The inner product between the observation matrix $\boldsymbol{\Psi}$ and the residue $\mathbf{r}$ has the complexity of $\mathcal{O}(GN)$; the equivalent LS problem $\Delta\hat{\mathbf{e}}_i^{(k)}|_{\Gamma_t} \leftarrow \boldsymbol{\Psi}^{\dagger}_{\Gamma_t}\Delta\mathbf{q}_i$ requires the complexity $\mathcal{O}(GK_N)$. The average total number of iterations is reduced from K_N in SAMP to $K_N - K_N^{(0)}$ in PA-SAMP; therefore, the total complexity of PA-SAMP is in the order of $\mathcal{O}((K_N - K_N^{(0)})GN)$ (note that $K_N \ll N$), reducing the complexity of SAMP by a factor of $K_N^{(0)}/K_N$. To sum up, the total complexity of the proposed NBI cancelation approach is on the order of $\mathcal{O}(N\log_2(N) + (K_N - K_N^{(0)})GN)$.

Similarly, the computational complexity of the proposed CS-based IN cancelation scheme mainly contains the *a priori* information acquisition with the complexity of $\mathcal{O}(N)$ and the PA-SAMP algorithm for IN recovery with the complexity of $\mathcal{O}((K_I - K_I^{(0)})RN)$. Hence, the total complexity for IN cancelation is $\mathcal{O}(N + (K_I - K_I^{(0)})RN)$.

B. RIP Performance Evaluation

The observation matrix should satisfy the restricted isometry property (RIP) to solve the CS problem accurately according to the probabilistic theory of sparse signal recovery [43]. It can be verified through numerical calculation analysis that the observation matrix $\mathbf{F}_G$ of the proposed NBI recovery approach satisfies the RIP property well with the $2K_N$-RIP constant $\delta_{2K_N} < 0.362$ when the sparsity level $K_N = 10$. Meanwhile, the observation matrix $\mathbf{F}_R$ for the IN recovery approach satisfies the RIP property with $\delta_{2K_I} < 0.384$ when the sparsity level $K_I = 15$. This implies that the K_N-sparse NBI and the K_I-sparse IN can be successfully recovered within the AWGN error bound using the proposed schemes, according to the RIP constraint that δ_{2K_N} and δ_{2K_I} are required to be less than 0.41 [43].

V. Simulation Results and Discussions

The performance of the proposed CS-based simultaneous NBI and IN cancelation schemes for wireless vehicular communications scenario is investigated and validated through extensive simulations. The signal bandwidth is configured as 7.56 MHz located at the central frequency of 6 GHz [44]. The Vehicular B channel model [45] widely used to emulate the wireless vehicular channel is applied. The OFDM subcarrier number $N = 1024$, the length of each TS $M = 128$, and the number of null subcarriers $R = 128$ are adopted. The modulation scheme 64-QAM in low-speed vehicular channels with the relative receiver velocity of 30 km/h is considered. To make the vehicular transmission more dependable, the effective channel code of low-density parity check (LDPC) with code length of 64 800 bits, and code rate of 2/3 [37] is adopted. As described in Section II-A, the NBI is modeled by the superposition of independent tone interferers with INR = 32 dB. The sparsity level is invariable for each simulation, whereas the support may vary randomly with a uniform distribution $U[0, N-1]$ at all the N subcarriers. The IN arrival rate is described by Poisson process with a medium value of $\lambda = 50/s$, and the instantaneous amplitude of the IN is modeled by the Middleton's Class A distribution with the parameters $A = 0.15$ and $\omega = 0.02$.

The general process of the proposed approach for NBI and IN recovery is shown in Fig. 2 with $K_N = 10$ and $K_I = 10$. It can be noted from Fig. 2(a) and (b) that the final NBI and IN estimations using the PA-SAMP algorithm accurately match the actual NBI and IN, respectively.

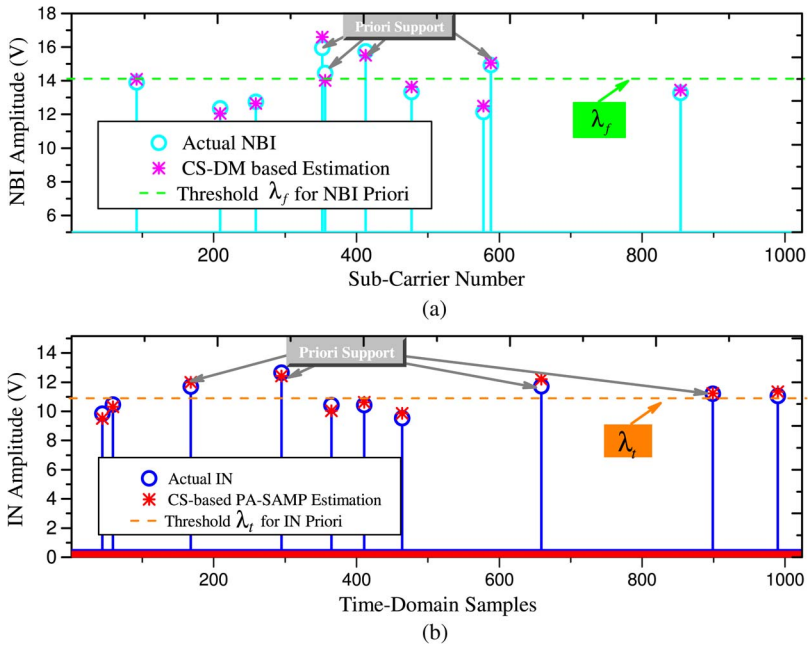

Fig. 2. NBI and IN recovery process using the proposed PA-SAMP algorithm.

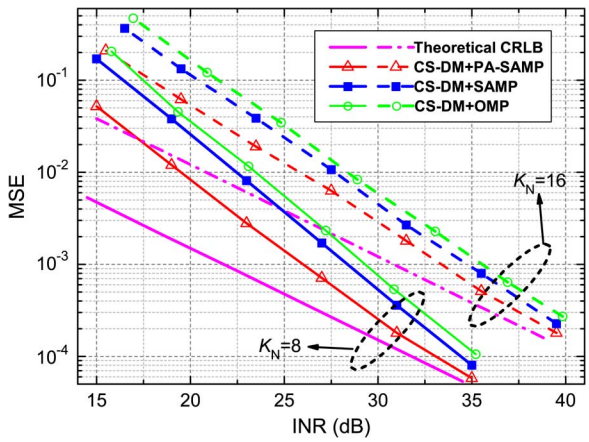

Fig. 3. MSE performance comparisons for NBI reconstruction using CS-DM with PA-SAMP and SAMP under the Vehicular B channel.

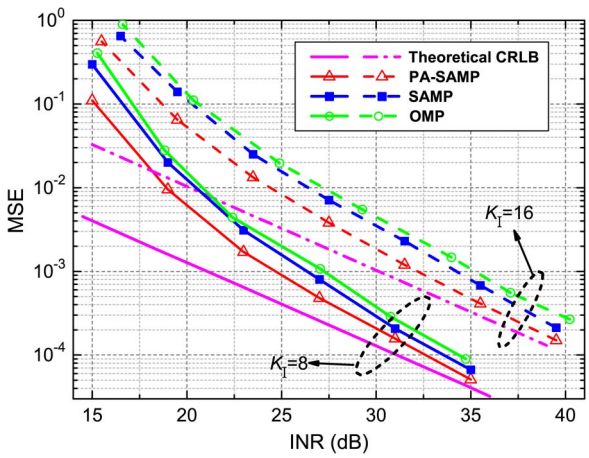

Fig. 4. MSE performance comparisons for IN reconstruction using PA-SAMP and SAMP under the Vehicular B channel.

The MSE performances of NBI and IN recovery using the proposed method are shown in Figs. 3 and 4, respectively. The theoretical Cramer–Rao lower bounds (CRLBs) $2\sigma_w^2 \cdot (N \cdot K_N/G)$ and $2\sigma_w^2 \cdot (N \cdot K_I/R)$ [46] for NBI and IN, respectively, are also included for comparison. In Fig. 3, the performance of the CS-DM scheme for NBI recovery with the greedy algorithms of PA-SAMP, SAMP [25], and the classical OMP [41] (assuming that the sparsity level is known for OMP to make the performance of OMP comparable) are shown for the sparsity level $K_N = 8$ and $K_N = 16$. The PA-SAMP algorithm achieves a target MSE of 10^{-3} at the INR of 26.3 and 33.1 dB with the sparsity level $K_N = 8$ and $K_N = 16$, respectively, which outperforms SAMP and OMP by approximately 1.7 and 2.0 dB, respectively. Fig. 4 shows the MSE performance of the CS-based IN recovery scheme. The PA-SAMP algorithm achieves the MSE 10^{-3} at the INR of 24.6 and 32.3 dB with $K_I = 8$ and $K_I = 16$, respectively, which outperforms SAMP and OMP by approximately 1.8 and 2.2 dB, respectively. It is noted from Figs. 3 and 4 that the MSE of the proposed methods approach the theoretical CRLB with the increase in the INR; therefore, the high accuracy of the proposed simultaneous NBI and IN cancelation method is verified for vehicular communications.

To quantitatively measure the execution time of PA-SAMP and SAMP to validate the complexity analysis in Section IV, the average number of iterations using PA-SAMP and SAMP for NBI reconstruction is summarized in Table I, where the average value is calculated from 10^6 times of NBI reconstruction simulations. It can be noted that the average iteration number to reach the same criterion (MSE $< 10^{-3}$, INR $= 32$ dB) for PA-SAMP is significantly smaller than that of SAMP in the case of different sparsity levels.

TABLE I
AVERAGE NUMBER OF ITERATIONS TO REACH SUCCESSFUL NBI RECONSTRUCTION

Sparsity Level	PA-SAMP	SAMP
4	1.74	3.36
8	4.02	7.14
16	11.58	16.33

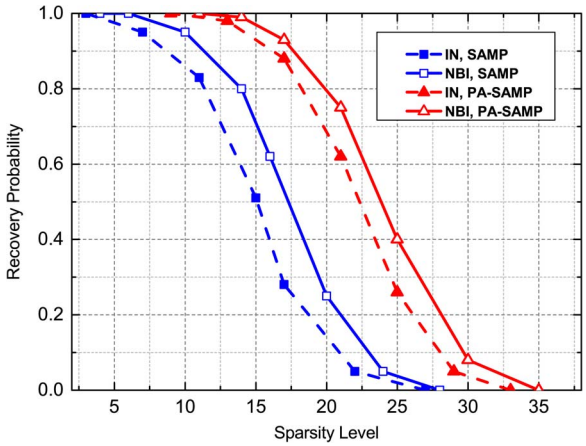

Fig. 5. Probability of NBI and IN recovery using PA-SAMP and SAMP under the Vehicular B channel.

The recovery probability of the proposed simultaneous NBI and IN recovery method versus different sparsity levels with the fixed INR of 32 dB under the Vehicular B channel is depicted in Fig. 5. The recovery probability is calculated by accumulating the number of MSE $< 10^{-2}$. The proposed simultaneous NBI and IN recovery method based on PA-SAMP reaches a successful recovery probability of 0.9 at the sparsity level of more than 16, which indicates that the proposed method based on PA-SAMP correctly recovers the NBI and IN at large sparsity levels from only a small portion of acquired measurement vector. For the NBI and IN in vehicular communications scenarios, the nonzero entries' ratio is commonly from 1% to 2% [2], [22], and the sparsity level is about in the range of 10 to 20 in this case, which indicates the effectiveness of the proposed PA-SAMP algorithm in practice. It is also noted from the gap between the curves of PA-SAMP- and SAMP-based methods that the proposed PA-SAMP method can accurately recover NBI and IN with the aid of partial support.

The bit-error-rate (BER) performance of the proposed simultaneous NBI and IN cancelation scheme under the Vehicular B channel with the NBI of $K_N = 10$, the IN of $K_I = 10$, and INR $= 32$ dB is shown in Fig. 6. The LDPC code with the code rate of 2/3 and 64-QAM are configured, which is the primary working mode of DTTB to provide high-definition TV services for vehicles in mobile scenarios [36]. The BER performances of the conventional non-CS-based method (FTE [12] along with clipping and blanking [47]) and the proposed CS-DM method with the classical algorithm SAMP are presented for comparison. The worst case ignoring NBI and IN, and the ideal case without NBI or IN are also depicted as benchmarks. It can be found that at the target BER of 10^{-4}, the proposed

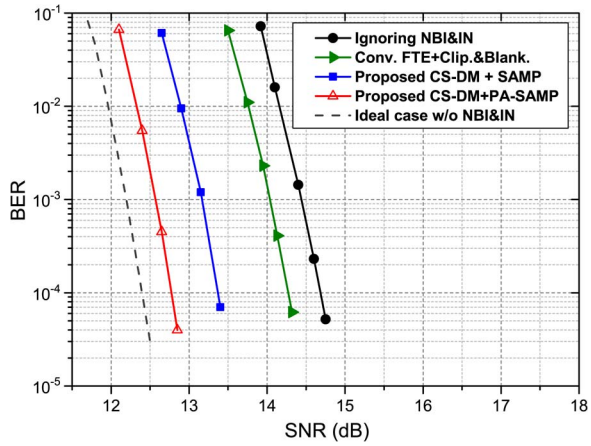

Fig. 6. BER performance comparison of different schemes under the Vehicular B channel with NBI and IN.

CS-DM method with the proposed algorithm PA-SAMP outperforms the proposed CS-DM method with classical SAMP, the conventional non-CS-based method, and the case ignoring NBI and IN by approximately 0.61, 1.57, and 2.0 dB, respectively. Furthermore, the gap between the proposed method and the ideal case without NBI and IN is only about 0.39 dB, validating the accuracy and effectiveness of the proposed simultaneous NBI and IN recovery method.

VI. CONCLUSION

In this paper, a novel CS-based simultaneous NBI and IN cancelation scheme to support reliable and high-speed vehicular communications is proposed, and its performance is validated by theoretical analysis and simulations. Under the proposed framework of CS-TFM-OFDM, the proposed CS-DM method acquires the CS measurement vector of the NBI exploiting the temporal repeated TSs. Then, the NBI is accurately recovered through the proposed PA-SAMP algorithm with the aid of the *a priori* partial support. Meanwhile, the IN is accurately reconstructed from the measurement vector at the null subcarriers using PA-SAMP. The NBI and IN signals are separately and accurately recovered with low complexity, which outperforms conventional counterparts. Hence, the NBI and IN that have severe impacts on the stability of vehicular communications are *double killed*. In addition, the proposed CS-TFM-OFDM framework is as spectrum efficient as CP-OFDM. The current vehicular standards can adopt the proposed methods to solve the mitigation problem of NBI or IN. Furthermore, the proposed frame structure CS-TFM-OFDM will overcome the limitation of using current standards and can be possibly adopted in future vehicular standards or other communications systems suffering from NBI and IN.

REFERENCES

[1] N. Navet, Y. Song, F. Simonot-Lion, and C. Wilwert, "Trends in automotive communication systems," in *Proc. IEEE*, vol. 93, no. 6, pp. 1204–1223, Jun. 2005.
[2] S. Hasan, X. Ding, N. Siddique, and S. Chakraborty, "Measuring disruption in vehicular communications," *IEEE Trans. Veh. Technol.*, vol. 60, no. 1, pp. 148–159, Jan. 2011.

[3] F. Yang, K. Yan, Q. Xie, and J. Song, "Non-equiprobable APSK constellation labeling design for BICM systems," *IEEE Commun. Lett.*, vol. 17, no. 6, pp. 1276–1279, Jun. 2013.
[4] F. Yang, K. Yan, C. Pan, and J. Song, "PAPR reduction for systems using SRRC filters based on modified ACE," *IEICE Trans. Fundam.*, vol. E96-A, no. 7, pp. 1675–1677, Jul. 2013.
[5] *IEEE Standard for Information technology—Local and metropolitan area networks- Specific requirements–Part 11: Wireless LAN Medium Access Control (MAC) and Physical Layer (PHY) Specifications Amendment 6: Wireless Access in Vehicular Environments*, IEEE Std. 802.11p, Jul. 2010.
[6] *HomePlug Green PHY The Standard For In-Home Smart Grid Powerline Communications*, HomePlug Alliance Std., Jun. 2010.
[7] S. L. Primak and V. Z. Lyandres, "On the generation of the baseband and narrowband non-Gaussian processes," *IEEE Trans. Signal Process.*, vol. 46, no. 5, pp. 1229–1237, May 1998.
[8] A. Nasri and R. Schober, "Robust L_p-norm decoding for BICM-based secondary user systems," *IEEE Trans. Commun.*, vol. 58, no. 11, pp. 3084–3090, Nov. 2010.
[9] M. Marey and H. Steendam, "Analysis of the narrowband interference effect on OFDM timing synchronization," *IEEE Trans. Signal Process.*, vol. 55, no. 9, pp. 4558–4566, Sep. 2007.
[10] J. Park, D. Kim, C. Kang, and D. Hong, "Effect of bluetooth interference on OFDM-based WLAN," in *Proc. IEEE Veh. Technol. Conf.*, Oct. 2003, vol. 2, pp. 786–789.
[11] R. Shepherd, J. Gaddie, and D. Nielson, "New techniques for suppression of automobile ignition noise," *IEEE Trans. Veh. Technol.*, vol. 25, no. 1, pp. 2–12, Feb. 1976.
[12] S. Kai *et al.*, "Impacts of narrowband interference on OFDM-UWB receivers: Analysis and mitigation," *IEEE Trans. Signal Process.*, vol. 55, no. 3, pp. 1118–1128, Mar. 2007.
[13] A. Coulson, "Bit error rate performance of OFDM in narrowband interference with excision filtering," *IEEE Trans. Commun.*, vol. 5, no. 9, pp. 2484–2492, Sep. 2006.
[14] D. Darsena, "Successive narrowband interference cancellation for OFDM systems," *IEEE Commun. Lett.*, vol. 11, no. 1, pp. 73–75, Jan. 2007.
[15] F. Juwono, Q. Guo, D. Huang, and K. P. Wong, "Deep clipping for impulsive noise mitigation in OFDM-based power-line communications," *IEEE Trans. Power Del.*, vol. 29, no. 3, pp. 1335–1343, Jun. 2014.
[16] A. Dubey, R. Mallik, and R. Schober, "Performance analysis of a power line communication system employing selection combining in correlated log-normal channels and impulsive noise," *IET Commun.*, vol. 8, no. 7, pp. 1072–1082, May 2014.
[17] F. Abdelkefi, P. Duhamel, and F. Alberge, "Impulsive noise cancellation in multicarrier transmission," *IEEE Trans. Commun.*, vol. 53, no. 1, pp. 94–106, Jan. 2005.
[18] D. Donoho, "Compressed sensing," *IEEE Trans. Inf. Theory*, vol. 52, no. 4, pp. 1289–1306, Apr. 2006.
[19] W. Ding, F. Yang, C. Pan, L. Dai, and J. Song, "Compressive sensing based channel estimation for OFDM systems under long delay channels," *IEEE Trans. Broadcast.*, vol. 60, no. 2, pp. 313–321, Jun. 2014.
[20] A. Gomaa and N. Al-Dhahir, "A compressive sensing approach to NBI cancellation in mobile OFDM systems," in *Proc. IEEE GLOBECOM*, Dec. 2010, pp. 1–5.
[21] G. Caire, T. Al-Naffouri, and A. Narayanan, "Impulse noise cancellation in OFDM: An application of compressed sensing," in *Proc. IEEE ISIT*, Jul. 2008, pp. 1293–1297.
[22] T. Naffouri, A. Quadeer, and G. Caire, "Impulse noise estimation and removal for OFDM systems," *IEEE Trans. Commun.*, vol. 62, no. 3, pp. 976–989, Mar. 2014.
[23] *Wireless LAN Medium Access Control (MAC) and Physical Layer (PHY) Specifications*, IEEE Std. 802.11n, Oct. 2009.
[24] *IEEE Standard for Broadband over Power Line Networks: Medium Access Control and Physical Layer Specifications*, IEEE Std. 1901-2010, Dec. 2010.
[25] T. Do, G. Lu, N. Nguyen, and T. Tran, "Sparsity adaptive matching pursuit algorithm for practical compressed sensing," in *Proc. Asilomar Conf. Signals, Syst. Comput.*, Oct. 2008, pp. 581–587.
[26] A. Tonello and F. Pecile, "Efficient architectures for multiuser FMT systems and application to power line communications," *IEEE Trans. Commun.*, vol. 57, no. 5, pp. 1275–1279, May 2009.
[27] D. Umehara, H. Nishiyori, and Y. Morihiro, "Performance evaluation of CMFB transmultiplexer for broadband power line communications under narrowband interference," in *Proc. IEEE ISPLC*, 2006, pp. 50–55.
[28] A. Giorgetti, M. Chiani, and M. Win, "The effect of narrowband interference on wideband wireless communication systems," *IEEE Trans. Commun.*, vol. 53, no. 12, pp. 2139–2149, Dec. 2005.
[29] A. Coulson, "Narrowband interference in pilot symbol assisted OFDM systems," *IEEE Trans. Wireless Commun.*, vol. 3, no. 6, pp. 2277–2287, Nov. 2004.
[30] J. Zyren, "Homeplug green phy overview," Atheros Commun., San Diego, CA, USA, Tech. Paper, May 2010.
[31] A. Oka and L. Lampe, "Compressed sensing reception of bursty UWB impulse radio is robust to narrow-band interference," in *Proc. IEEE Globecom*, Nov. 2009, pp. 1–7.
[32] E. V. D. Berg and M. Friedlander, "Theoretical and empirical results for recovery from multiple measurements," *IEEE Trans. Inf. Theory*, vol. 56, no. 5, pp. 2516–2527, May 2010.
[33] F. Sacuto, F. Labeau, and B. Agba, "Wide band time-correlated model for wireless communications under impulsive noise within power substation," *IEEE Trans. Wireless Commun.*, vol. 13, no. 3, pp. 1449–1461, Mar. 2014.
[34] D. Middleton, "Non-Gaussian noise models in signal processing for telecommunications: New methods an results for class A and class B noise models," *IEEE Trans. Inf. Theory*, vol. 45, no. 4, pp. 1129–1149, May 1999.
[35] N. Andreadou and F. Pavlidou, "Modeling the noise on the OFDM power-line communications system," *IEEE Trans. Power Del.*, vol. 25, no. 1, pp. 150–157, Jan. 2010.
[36] *Error-Correction, Data Framing, Modulation and Emission Methods for Digital Terrestrial Television Broadcasting*, Recommendation ITU-R BT. Std. 1306-6, Dec. 2011.
[37] *Digital Video Broadcasting (DVB); Frame Structure, Channel Coding and Modulation for a Second Generation Digital Terrestrial Television Broadcasting System (DVB-T2)*, ETSI EN Std. 302 755, Apr. 2012.
[38] D. Donoho, M. Elad, and V. Temlyakov, "Stable recovery of sparse overcomplete representations in the presence of noise," *IEEE Trans. Inf. Theory*, vol. 52, no. 1, pp. 6–18, Jan. 2006.
[39] M. Zimmermann and K. Dostert, "A multipath model for the powerline channel," *IEEE Trans. Commun.*, vol. 50, no. 4, pp. 553–559, Apr. 2002.
[40] E. Candes and T. Tao, "Decoding by linear programming," *IEEE Trans. Inf. Theory*, vol. 51, no. 12, pp. 4203–4215, Dec. 2005.
[41] J. Tropp and A. Gilbert, "Signal recovery from random measurements via orthogonal matching pursuit," *IEEE Trans. Inf. Theory*, vol. 53, no. 12, pp. 4655–4666, Dec. 2007.
[42] W. Dai and O. Milenkovic, "Subspace pursuit for compressive sensing signal reconstruction," *IEEE Trans. Inf. Theory*, vol. 55, no. 5, pp. 2230–2249, May 2009.
[43] J. Candès and Y. Plan, "A probabilistic and RIPless theory of compressed sensing," *IEEE Trans. Inf. Theory*, vol. 57, no. 11, pp. 7235–7254, Nov. 2011.
[44] S. Liu, F. Yang, W. Ding, and J. Song, "Structured compressive sensing based narrowband interference mitigation for vehicular communications," in *Proc. IEEE ICC*, Jun. 2015, pp. 2375–2380.
[45] *Guideline for Evaluation of Radio Transmission Technology for IMT-2000*, Recommendation ITU-R M. Std. 1225, 1997.
[46] S. Liu, F. Yang, and J. Song, "Narrowband interference cancelation based on priori aided compressive sensing for DTMB systems," *IEEE Trans. Broadcast.*, vol. 61, no. 1, pp. 66–74, Mar. 2015.
[47] S. Zhidkov, "Analysis and comparison of several simple impulsive noise mitigation schemes for OFDM receivers," *IEEE Trans. Commun.*, vol. 56, no. 1, pp. 5–9, Jan. 2008.

Sicong Liu (S'15) received the B.S.E. degree in electronic engineering from Tsinghua University, Beijing, China. He is currently working toward the Ph.D. degree in electronic engineering with the DTV Technology R&D Center, Research Institute of Information Technology, Tsinghua National Laboratory for Information Science and Technology, Tsinghua University.

His research interests include power line communications, broadband transmission techniques, and interference mitigation.

Fang Yang (M'11–SM'13) received the B.S.E. and Ph.D. degrees in electronic engineering from Tsinghua University, Beijing, China, in 2005 and 2009, respectively.

He is currently an Associate Professor with the DTV Technology R&D Center, Research Institute of Information Technology, Tsinghua National Laboratory for Information Science and Technology, Tsinghua University. His research interests include power line communications, visible-light communications, and digital television terrestrial broadcasting.

Wenbo Ding (S'15) received the B.S.E. degree (with distinction) in 2011 from Tsinghua University, Beijing, China, where he is currently working toward the Ph.D. degree with the DTV Technology R&D Center, Research Institute of Information Technology, Tsinghua National Laboratory for Information Science and Technology.

His research interests include sparse signal processing and its applications in the field of power line communications, visible light communications, smart grid, and future fifth-generation wireless communications. He is the author of over 20 journal and conference papers.

Mr. Ding received the IEEE Scott Helt Memorial Award for the Best Paper published in IEEE TRANSACTIONS ON BROADCASTING in 2015 and the Academic Star Award from the Department of Electronic Engineering, Tsinghua University, in 2015.

Jian Song (M'06–SM'10) received the B.Eng. and Ph.D. degrees in electrical engineering from Tsinghua University, Beijing, China, in 1990 and 1995, respectively.

In 1996, he was with The Chinese University of Hong Kong, Hong Kong, and, in 1997, with the University of Waterloo, Waterloo, ON, Canada. He was with Hughes Network Systems, Germantown, MD, USA, for seven years before joining the faculty team at Tsinghua University in 2005 as a Professor. He is currently the Director of DTV Technology R&D Center, Research Institute of Information Technology, Tsinghua National Laboratory for Information Science and Technology, Tsinghua University. He has been working in many different areas of fiber-optic, satellite, and wireless communications, as well as power-line communications. He is the author of more than 110 peer-reviewed journal and conference papers, He is a holder of two U.S. and more than 20 Chinese patents. His current research interests include digital TV broadcasting.

Dr. Song is a Fellow of the Institution of Engineering Technology.